

The coincidence problem and interacting holographic dark energy

Khamphée Karwan

Theoretical High-Energy Physics and Cosmology Group, Department of Physics,
Chulalongkorn University, Bangkok 10330, Thailand

Abstract. We study the dynamical behaviour of the interacting holographic dark energy model whose interaction term is $Q = 3H(\lambda_d\rho_d + \lambda_c\rho_c)$, where ρ_d and ρ_c are the energy density of dark energy and CDM respectively. To satisfy the observational constraints from SNIa, CMB shift parameter and BAO measurement, if $\lambda_c = \lambda_d$ or $\lambda_d, \lambda_c > 0$, the cosmic evolution will only reach the attractor in the future and the ratio ρ_c/ρ_d cannot be slowly varying at present. Since the cosmic attractor can be reached in the future even when the present values of the cosmological parameters do not satisfy the observational constraints, the coincidence problem is not really alleviated in this case. However, if $\lambda_c \neq \lambda_d$ and they are allowed to be negative, the ratio ρ_c/ρ_d can be slowly varying at present and the cosmic attractor can be reached near the present epoch. Hence, the alleviation of the coincidence problem is attainable in this case. The alleviation of coincidence problem in this case is still attainable when confronting this model to SDSS data.

Keywords: Dark Energy.

1. Introduction

Observations suggest that the expansion of the universe is accelerating [1, 2]. The acceleration of the universe may be explained by supposing that the present universe is dominated by a mysterious form of energy whose pressure is negative, known as dark energy. One problem of the dark energy model is the coincidence problem, which is the problem why the dark energy density and matter density are of the same order of magnitude in the present epoch although they differently evolve during the expansion of the universe. A possible way to alleviate the coincidence problem is to suppose that there is an interaction between matter and dark energy. The cosmic coincidence can then be alleviated by appropriate choice of the form of the interaction between matter and dark energy leading to a nearly constant ratio $r = \rho_c/\rho_d$ during the present epoch [3, 4, 5] or giving rise to attractor of the cosmic evolution at late time [6, 7]. Since the existence of the cosmic attractor implies constant r but the attractor does not always occur at the present epoch, we first find a range of dark energy parameters for which the attractor occurs and then check the evolution of r during the present epoch.

Based on holographic ideas [8, 9], one can determine the dark energy density in terms of the horizon radius of the universe. This type of dark energy is holographic dark energy [10] - [14]. By choosing Hubble radius as the cosmological horizon, the present amount of dark energy density agrees with observations. Nevertheless, dark energy evolves like matter at present, so it cannot lead to an accelerated expansion. However, if the particle horizon is chosen to be the cosmological horizon, the equation of state parameter of dark energy can become negative but not negative enough to drive an accelerating universe. The situation is better when one uses the event horizon as the cosmological horizon. In this case, dark energy can drive the present accelerated expansion, and the coincidence problem can be resolved by assuming an appropriate number of e-foldings of inflation. Roughly speaking, the coincidence problem can be resolved because the size of the cosmological horizon during the present epoch depends on the amount of e-folds of inflation, and the amount of holographic dark energy depends on the horizon size. Nevertheless, the second law of thermodynamics will be violated if $w_d < -1$ [9, 15]. Hence, w_d should not cross the boundary $w_d = -1$. The boundary $w_d = -1$ can be crossed if dark energy interacts with matter. Since now the horizon size has a dependence on the interaction terms, the alleviation of cosmic coincidence should also depend on the interaction term.

In this work we suppose that the holographic dark energy interact only with cold dark matter (CDM) and treat baryons as non-interacting matter component. Our objective is to compare the region of dark energy parameters for which the cosmic evolution has an attractor within the parameter region that satisfies the observational constraints from combined analysis of SNIa data [16], CMB shift parameter [17] and BAO measurement [18]. The results of the comparison can tell us about the range of parameters that alleviate the cosmic coincidence.

2. The autonomous equations

In this section, we derive the first order differential equations that describe the evolution of radiation, baryon, CDM and dark energy densities in the universe. By analyzing these equations, one can estimate the asymptotic evolution of the universe. To proceed, we start from the Friedmann equation

$$H^2 + \frac{K}{a^2} = \frac{1}{3\bar{m}_p} (\rho_r + \rho_b + \rho_c + \rho_d), \quad (1)$$

where H is the Hubble parameter and the subscripts r, b, c and d correspond to the radiation, baryons, CDM and dark energy respectively. The parameter K denotes the curvature of the universe, where $K = -1, 0, +1$ for the close, flat and open universe respectively. The above equation can be written in terms of the density parameters $\Omega_K = K/(a^2 H^2)$ and $\Omega_\alpha = \rho_\alpha/(3\bar{m}_p^2 H^2)$ as

$$1 + \Omega_K = \sum_{\alpha=r,b,c,d} \Omega_\alpha = \Omega_r + \Omega_b + \Omega_c + \Omega_d. \quad (2)$$

The index α runs over the 4 species, namely radiation, baryons, CDM and dark energy. We now derive the autonomous equations for the dynamical variables Ω_K and Ω_α . Differentiating $\Omega_K = K/(a^2 H^2)$ with respect to $\ln a$, we get

$$\Omega'_K = -\frac{2K}{H} \left(\frac{\dot{a}}{a^3 H^2} + \frac{\dot{H}}{a^2 H^3} \right) = -2\Omega_K \left(1 + \frac{\dot{H}}{H^2} \right), \quad (3)$$

where prime and dot denote derivative with respect to $\ln a$ and time respectively. From the definition of the density parameter, one can show that

$$\Omega'_\alpha = \Omega_\alpha \left(\frac{\dot{\rho}_\alpha}{H \rho_\alpha} - 2 \frac{\dot{H}}{H^2} \right). \quad (4)$$

To study the evolution of the universe at late time, we will search for the fixed points of the above autonomous equations and check the stability of these fixed points. The fixed points of eqs. (3) and (4) are the points $(\Omega_K, \Omega_\alpha)$ at which

$$\Omega'_K = \Omega'_\alpha = 0. \quad (5)$$

It follows from eq. (3) that $\Omega'_K = 0$ at $\Omega_K = 0$ or $1 + \dot{H}/H^2 = 0$. Hence, possible fixed points at $\Omega_K \neq 0$ correspond to the non-accelerating universe, i.e. $1 + \dot{H}/H^2 \propto \ddot{a} = 0$. Since the expansion of the universe is accelerating today, we consider only the fixed points at $\Omega_K = 0$, and therefore neglect Ω_K in our consideration for simplicity.

Now we come to the case of interacting holographic dark energy and use eq. (4) to obtain the autonomous equation for this case. In the holographic dark energy scenario, the energy density of dark energy is related to the cosmological horizon L by

$$\rho_d = 3c^2 \bar{m}_p^2 L^{-2}, \quad (6)$$

where c is a positive constant. Differentiating the above equation with respect to time, we obtain

$$\dot{\rho}_d = -2\rho_d \frac{\dot{L}}{L}. \quad (7)$$

We take the cosmological horizon to be the event horizon, which is defined as $R_e(t) = a(t) \int_t^\infty d\tilde{t}/a(\tilde{t})$. Hence,

$$\frac{\dot{L}}{L} = \frac{\dot{R}_e}{R_e} = H - \frac{1}{R_e}. \quad (8)$$

We therefore get

$$\dot{\rho}_d = -2H\rho_d + 2\frac{\rho_d^{3/2}}{\sqrt{3c\bar{m}_p}}. \quad (9)$$

When dark energy has an interaction with CDM, the continuity equations yield

$$\dot{\rho}_c = -3H\rho_c + Q, \quad (10)$$

$$\dot{\rho}_d = -3H(1+w_d)\rho_d - Q, \quad (11)$$

where $Q = 3H(\lambda_d\rho_d + \lambda_c\rho_c)$. Usually, one supposes that $Q > 0$ because the second law of thermodynamics might be violated if energy transfers from matter to dark energy ($Q < 0$). However, for generality, we will not restrict Q to be positive in our consideration. Comparing eq. (9) with eq. (11), we get

$$w_d = -\frac{1}{3} - 2\frac{\sqrt{\Omega_d}}{3c} - \frac{\lambda_d\Omega_d + \lambda_c\Omega_c}{\Omega_d}. \quad (12)$$

We assume that radiation and baryons have no interaction with dark energy, so that they obey the continuity equations

$$\dot{\rho}_r = -4H\rho_r \quad \text{and} \quad \dot{\rho}_b = -3H\rho_b. \quad (13)$$

From eq. (1), one can show that

$$2\frac{\dot{H}}{H^2} = \frac{(H^2)^\cdot}{H^3} = -3 + \Omega_d + 2\frac{\Omega_d^{3/2}}{c} + 3(\lambda_d\Omega_d + \lambda_c\Omega_c) - \Omega_r. \quad (14)$$

In the above equation, we set $\Omega_K = 0$. Using eqs. (4), (9), (13) and (14), we obtain

$$\Omega'_d = \Omega_d \left(1 + 2\frac{\Omega_d^{1/2}}{c} - \Omega_d - 2\frac{\Omega_d^{3/2}}{c} - 3(\lambda_d\Omega_d + \lambda_c\Omega_c) + \Omega_r \right), \quad (15)$$

$$\Omega'_c = \Omega_c \left(\frac{3}{\Omega_c}(\lambda_d\Omega_d + \lambda_c\Omega_c) - \Omega_d - 2\frac{\Omega_d^{3/2}}{c} - 3(\lambda_d\Omega_d + \lambda_c\Omega_c) + \Omega_r \right), \quad (16)$$

$$\Omega'_r = \Omega_r \left(-1 - \Omega_d - 2\frac{\Omega_d^{3/2}}{c} - 3(\lambda_d\Omega_d + \lambda_c\Omega_c) + \Omega_r \right), \quad (17)$$

$$\Omega'_b = \Omega_b \left(-\Omega_d - 2\frac{\Omega_d^{3/2}}{c} - 3(\lambda_d\Omega_d + \lambda_c\Omega_c) + \Omega_r \right). \quad (18)$$

The fixed points of the above equations are $(\Omega_d, \Omega_c, \Omega_r, \Omega_b) = (0, 0, \Omega_{rc}, 0)$, $(0, 0, 0, \Omega_{bc})$ and $(\Omega_{dc}, \Omega_{cc}, 0, 0)$. Since we are interested in the late time evolution of the universe, we will consider only the fixed point $(\Omega_{dc}, \Omega_{cc}, 0, 0)$. This fixed point can occur at late time, i.e., about the present or in the future, because Ω_r/Ω_c usually decreases with time and

Ω_b/Ω_c can decrease with time if $Q > 0$. Using eqs. (15) and (16), the relation between Ω_{dc} and Ω_{cc} can be written as

$$1 + 2\frac{\Omega_{dc}^{1/2}}{c} = \frac{3}{\Omega_{cc}}(\lambda_d\Omega_{dc} + \lambda_c\Omega_{cc}). \quad (19)$$

From eq. (2), we have $\Omega_{dc} + \Omega_{cc} = 1$ and hence

$$1 - 3\lambda_c + 2\frac{\Omega_{dc}^{1/2}}{c} - (1 + 3\lambda_d - 3\lambda_c)\Omega_{dc} - 2\frac{\Omega_{dc}^{3/2}}{c} = 0. \quad (20)$$

The solution of eq. (20) gives Ω_{dc} in terms of λ_d , λ_c and c . Instead of finding the solution of this equation, we will use eq. (19) to compute the cosmological parameters of interest in the following section. The basic idea is that there are various values of c , λ_d and λ_c that satisfy eq. (19) for given Ω_{dc} and Ω_{cc} . Changes in the values of c , λ_d and λ_c lead to a different cosmological evolutions, i.e. a different w_d for a given Ω_{dc} and Ω_{cc} .

The stability of this fixed point can be investigated by linearizing eqs. (15) - (18) around the fixed point and studying how the fluctuations around the fixed point evolve in time. If the amplitude of the fluctuations decreases in time, the fixed point is a stable fixed point or attractor. Linearizing eqs. (15) - (18) around $(\Omega_{dc}, \Omega_{cc}, 0, 0)$, we get

$$\delta\Omega'_d = \left(\frac{\Omega_{dc}^{1/2}}{c} - \Omega_{dc} - 3\frac{\Omega_{dc}^{3/2}}{c} - 3\lambda_d\Omega_{dc} \right) \delta\Omega_d - 3\lambda_c\Omega_{dc}\delta\Omega_c + \Omega_{dc}\delta\Omega_r, \quad (21)$$

$$\delta\Omega'_c = \left(-1 - 2\frac{\Omega_{dc}^{1/2}}{c} + 3\lambda_c\Omega_{dc} \right) \delta\Omega_c + \left(3\lambda_d - \Omega_{cc} - 3\Omega_{cc}\frac{\Omega_{dc}^{1/2}}{c} - 3\lambda_d\Omega_{cc} \right) \delta\Omega_d + \Omega_{cc}\delta\Omega_r, \quad (22)$$

$$\delta\Omega'_r = -2 \left(1 + \frac{\Omega_{dc}^{1/2}}{c} \right) \delta\Omega_r, \quad (23)$$

$$\delta\Omega'_b = - \left(1 + 2\frac{\Omega_{dc}^{1/2}}{c} \right) \delta\Omega_b, \quad (24)$$

where $\delta\Omega_\alpha = \Omega_\alpha - \Omega_{\alpha c}$ denote fluctuations around the fixed point. The above linear equations can be written as

$$\delta\Omega'_\alpha = M_{\alpha\beta}\delta\Omega_\beta, \quad (25)$$

where α and β run over the 4 species. The eigenvalues of the matrix M govern how the amplitude of the fluctuations around the fixed point changes with time. The fixed point is a stable, saddle or unstable point if all the eigenvalues are negative, some of eigenvalues are positive or all the eigenvalues are positive, respectively. (Since we are dealing with real eigenvalues.) The eigenvalues of the matrix M are

$$\begin{aligned} \lambda_1 &= \frac{\Omega_{dc}^{1/2}}{c} - (1 + 3\lambda_d - 3\lambda_c)\Omega_{dc} - 3\frac{\Omega_{dc}^{3/2}}{c}, \\ \lambda_2 &= \lambda_4 = -1 - 2\frac{\Omega_{dc}^{1/2}}{c}, \quad \lambda_3 = -2 \left(1 + \frac{\Omega_{dc}^{1/2}}{c} \right). \end{aligned} \quad (26)$$

Hence, the fixed point $(\Omega_{dc}, \Omega_{cc}, 0, 0)$ is a stable point when $\lambda_1 < 0$ and a saddle point when $\lambda_1 > 0$. Using eq. (19), λ_1 can be written as

$$\lambda_1 = \frac{3(\lambda_d \Omega_{dc} + \lambda_c \Omega_{cc})}{\Omega_{cc}} \left(\frac{1}{2} - \Omega_{dc} \right) - \frac{1}{2} - \frac{\Omega_{dc}^{3/2}}{c} - 3(\lambda_d - \lambda_c) \Omega_{dc}. \quad (27)$$

It is not easy to determine the sign of λ_1 in general. Thus, we will determine it in particular cases in the next section.

3. The attractor of cosmic evolution

We now consider the fixed point and stability of the cosmic evolution around the present epoch. For simplicity, we first consider the case where $\lambda_d = \lambda_c = b^2$. In this case, eq. (19) becomes

$$1 + 2 \frac{\Omega_{dc}^{1/2}}{c} = \frac{3b^2}{\Omega_{cc}}. \quad (28)$$

Since $c > 0$, eq. (28) implies that $b^2 \geq \Omega_{cc}/3$. This is the lower limit of b^2 for the existence of the fixed point. From eqs. (12) and (28), it is easy to show that

$$w_d = -\frac{b^2}{\Omega_{cc}\Omega_{dc}}. \quad (29)$$

The equation of state parameter of the universe is defined as

$$w = \frac{p_{\text{total}}}{\rho_{\text{total}}} = \sum_{\alpha=r,b,m,d} w_{\alpha} \Omega_{\alpha}, \quad (30)$$

where $w_{\alpha} = p_{\alpha}/\rho_{\alpha}$. Since $w_b = w_c = 0$ and Ω_r can be neglected at late time, we have $w = w_d \Omega_d$ and therefore.

$$w = -\frac{b^2}{\Omega_{cc}}. \quad (31)$$

From the lower bound of b^2 , we get $w \leq 1/3$. This means that the fixed point corresponds to cosmic acceleration. Moreover, one can see that the universe will be in the phantom phase, i.e., $w < -1$, if $b^2 > \Omega_{cc}$ or equivalently $\Omega_{dc}^{1/2} > c$. Since the observations seem to indicate that $w_d < -1$ today, we find the value of b^2 that makes $w_d < -1$ at the fixed point. It follows from eq. (29) that $w_d < -1$ if $b^2 > \Omega_{cc}\Omega_{dc}$. We now check the stability of the fixed point. In this case, eq. (27) becomes

$$\lambda_1 = \frac{3b^2}{\Omega_{cc}} \left(\frac{1}{2} - \Omega_{dc} \right) - \frac{1}{2} - \frac{\Omega_{dc}^{3/2}}{c}. \quad (32)$$

It can be seen that it is not easy to find a point at which λ_1 changes sign. However, λ_1 is negative for any b^2 or c if $\Omega_{dc} > 1/2$, i.e. $\Omega_{dc} > \Omega_{cc}$. This means that the fixed point at which $\Omega_{dc} > \Omega_{cc}$ is a stable fixed point or attractor. Since the fixed point will occur when Q is positive and $\Omega_r = \Omega_b = 0$. At the present epoch Ω_r is small and can be neglected and with positive Q the ratio Ω_b/Ω_c decreases with time, so the fixed point $(\Omega_{dc}, \Omega_{cc}, 0, 0)$ will be reached in the future. From eqs. (15) - (18), one can see that if b^2 is large, Ω_b can decrease quickly with time compared with Ω_c . As a result, the fixed point

can be reached quickly near the present epoch. However, the CDM dominated epoch will disappear and the baryon fraction will be larger than the CDM fraction in the last scattering epoch due to the rapid decrease of ρ_b/ρ_c with time. This is excluded by the observed peak height ratio of the CMB power spectrum. Thus, based on observations, the fixed point cannot be reached near the present for this case. We will see in the next section that small b^2 or equivalently small Ω_{cc} is required by observations. Substituting $\Omega_{cc} = 1 - \Omega_{dc}$ into eq. (28), we get

$$1 - 3b^2 + 2\frac{\Omega_{dc}^{1/2}}{c} - \Omega_{dc} - 2\frac{\Omega_{dc}^{3/2}}{c} = 0 \quad (33)$$

The above third degree polynomial for $\Omega_{dc}^{1/2}$ will have one positive real root if $1 > 3b^2$. This root is the previously considered fixed point. In contrast, if $1 \leq 3b^2$ the above equation will have one additional real root. This root gives another fixed point at smaller Ω_{dc} . It is not hard to show that this fixed point is not stable and we will not consider it here.

Let us now consider the case where $\lambda_d \neq \lambda_c$. In this case, eq. (19) becomes

$$1 + 2\frac{\Omega_{dc}^{1/2}}{c} = \frac{3}{\Omega_{cc}} (\lambda_d \Omega_{dc} + \lambda_c \Omega_{cc}). \quad (34)$$

Hence, the fixed point occurs when $\lambda_d \Omega_{dc} + \lambda_c \Omega_{cc} > \Omega_{cc}/3$. Using eqs. (12) and (34), we get

$$w_d = -\frac{\lambda_d \Omega_{dc} + \lambda_c \Omega_{cc}}{\Omega_{cc} \Omega_{dc}}, \quad (35)$$

and therefore

$$w = -\frac{\lambda_d \Omega_{dc} + \lambda_c \Omega_{cc}}{\Omega_{cc}}. \quad (36)$$

Similarly to the case when $\lambda_d = \lambda_c$, one can show that the fixed point occurs when $w_d < -1/(3\Omega_{dc})$ or $w < -1/3$. Since the terms $\lambda_d \Omega_{dc}$ and $\lambda_c \Omega_{cc}$ from the interaction dominate at different times, the parameters λ_d and λ_c can be chosen such that the baryon fraction is smaller than the CDM fraction during the last scattering epoch although Ω_{cc} need not be very small. Thus, in this case, the attractor can be reached faster than the case of $\lambda_c = \lambda_d$. From eq. (27), we see that the fixed point is the stable fixed point when $\Omega_{dc} > \Omega_{cc}$ and λ_c is not much larger than λ_d .

4. The observational constraints

We now check the range of parameters for which the cosmic evolution has an attractor for compatibility with observations. We constrain the parameters of the interacting holographic dark energy using the latest observational data of SNIa [16] combined with the CMB shift parameter derived from three-year WMAP [17] and the baryon acoustic oscillations (BAO) from SDSS LRG [18].

The SNIa observations measure the apparent magnitude m of a supernova and its redshift z . The apparent magnitude m is related to the distance modulus μ and luminosity distance d_L of the supernova by

$$\mu(z) = m(z) - M = 5 \log_{10}(d_L(z)/\text{Mpc}) + 25, \quad (37)$$

where M is the absolute magnitude of the supernova. For flat space time, the luminosity distance is given by

$$d_L(z) = H_0^{-1}(1+z) \int_0^z \frac{d\tilde{z}}{E(\tilde{z})}. \quad (38)$$

Here, H_0 is the present value of the Hubble parameter and $E(z) = H(z)/H_0$. To constrain the holographic dark energy model, we perform χ^2 fit for the parameters $\lambda_d, \lambda_c, c, \Omega_{c0}, \Omega_{b0}$, where the subscript 0 denotes the present value. For Ω_{r0} , we compute its value from the CMB and Neutrino temperatures. Using eq. (2), one can compute Ω_{d0} from Ω_{c0}, Ω_{b0} and Ω_{r0} . We have to include radiation in our consideration because it should not be neglected when we compute CMB shift parameter. For the SNIa data, the parameter H_0 is the nuisance parameter which needs to be marginalized out. Since the fit of holographic dark energy to SNIa data is sensitive to H_0 [19], we have to add constraints from other observations to improve the fit. For this reason, we include the constraints from CMB shift parameter and BAO measurement in our analysis.

The CMB shift parameter is a quantity derived from CMB data that has been shown to be model independent, so it can be used to constrain cosmological models. The CMB shift parameter is defined as [20]

$$R = \Omega_{m0}^{1/2} \int_0^{z_{\text{CMB}}} \frac{d\tilde{z}}{E(\tilde{z})}, \quad (39)$$

where $\Omega_{m0} = \Omega_{c0} + \Omega_{b0}$ and $z_{\text{CMB}} = 1089$ is the redshift at recombination. The estimated value of R from 3-year WMAP data is 1.70 ± 0.03 . From the SDSS data, the measurement of the BAO peak in the distribution of SDSS LRG can be used to derive the model independent parameter A which is defined as [18]

$$A = \Omega_{m0}^{1/2} E(z_{\text{BAO}})^{-1/3} \left[\frac{1}{z_{\text{BAO}}} \int_0^{z_{\text{BAO}}} \frac{d\tilde{z}}{E(\tilde{z})} \right]^{2/3}, \quad (40)$$

where $z_{\text{BAO}} = 0.35$. The estimated A is $A = 0.469(n_s/0.98)^{-0.35} \pm 0.017$. According to the 3-year WMAP data, the scalar spectral index is chosen to be $n_s = 0.95$.

We first consider the case where $\lambda_d = \lambda_c = b^2$. For simplicity, we start by neglecting baryons in our consideration. Hence the attractor becomes $(\Omega_d, \Omega_c, \Omega_r) = (\Omega_{dc}, \Omega_{cc}, 0)$, where Ω_{dc} and Ω_{cc} satisfy eq. (28). The region of b^2 and Ω_{cc} for which the fixed point exists and the 99.7% confidence regions from the combined constraints are shown in figure 1. From this figure, one sees that a small b^2 is required by observations, so that the attractor that satisfies the observational constraints occurs at low Ω_{cc} . This implies that the attractor cannot occur at present at which $\Omega_c \approx 0.3$. In the future, Ω_c can become small, so that the fixed point can exist. Nevertheless, if the attractor is reached in the far future, the cosmic coincidence may not be alleviated because the present value of Ω_c

and w_d may not satisfy the observational constraints. In the following consideration, we will study how the ratio r evolves during the present epoch to check the possibility of alleviating the cosmic coincidence. Since the physical fixed point cannot occur if $b^2 < 0$, we perform another fit by supposing that $b^2 \geq 0$. The result is shown in figure 1. It can be seen that the above conclusions for the case of arbitrary b^2 are also valid for the case of $b^2 \geq 0$.

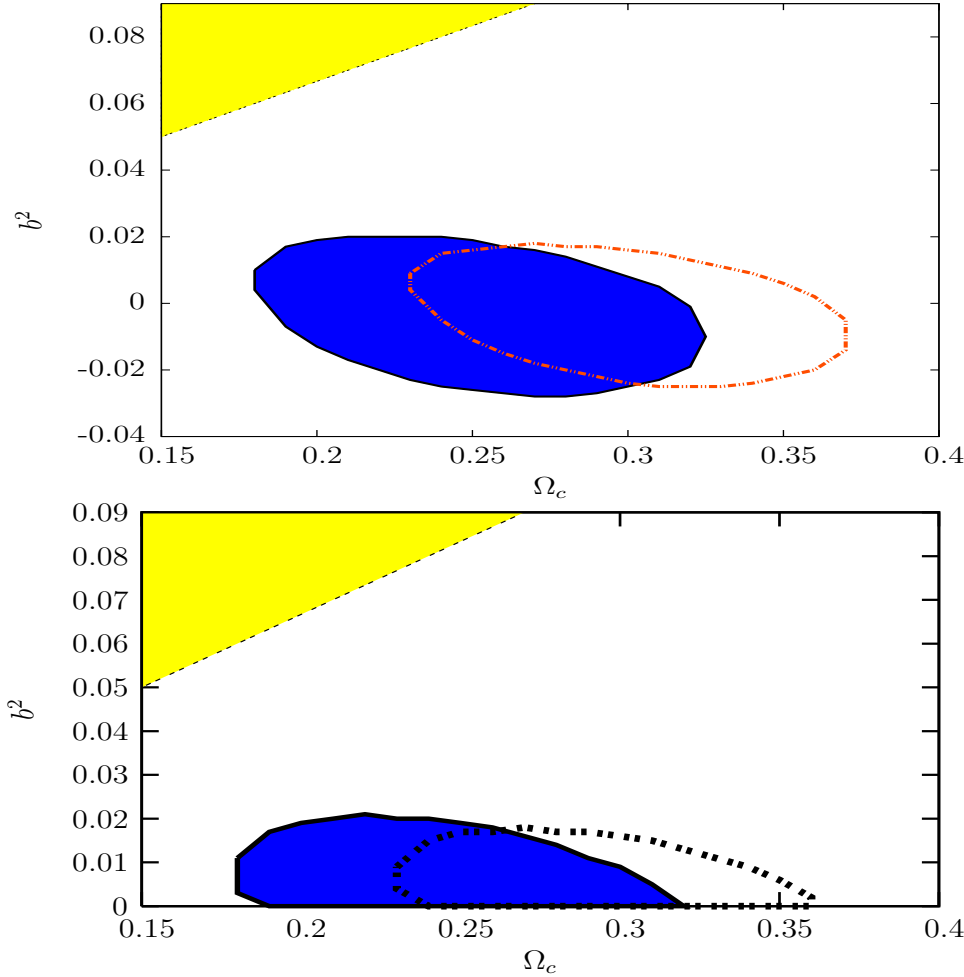


Figure 1. A region of parameters b^2 and Ω_c in which the cosmic evolution has a late time attractor (the yellow regions above the dashed lines), and the 99.7% confidence levels from the combined analysis of SNIa data, CMB shift parameter and BAO measurement. For the yellow region, Ω_c refers to Ω_{cc} , but Ω_c refers to Ω_{c0} for the confidence levels. The upper panel shows the case of arbitrary b^2 , while the lower panel shows the case where $b^2 \geq 0$. The blue regions represent the confidence regions for the case that includes baryons and prior $\Omega_{b0} = 0.047 \pm 0.006$, while the thick dotted lines represent the confidence levels for the case where baryons are neglected.

The situation changes a bit when we include baryons in our consideration. From the previous section, we know that the cosmic evolution reaches the attractor at $(\Omega_d, \Omega_c, \Omega_b, \Omega_r) = (\Omega_{dc}, \Omega_{cc}, 0, 0)$. Since the present value of Ω_b does not vanish, this attractor cannot occur at present. However, the attractor can occur in the future because the ratio Ω_b/Ω_c decreases with time due to the positive Q . It can be seen that the ratio

Ω_b/Ω_c decreases faster when b^2 increases. According to the observational constraints, a small b^2 is also required in this case, so that the attractor is slowly reached in the future. In order to perform a fit for this case, we use a prior $\Omega_{b0} = 0.047 \pm 0.006$ from the 1-year WMAP data [21] because Ω_{b0} cannot be constrained very well by using only SNIa data, CMB shift parameter and BAO measurement. It can be seen from figure 1 that the shape of the confidence contours does not change much when we include non-interacting baryons in our consideration. Obviously, the contours move to the left when the amount of Ω_{b0} increases. This is because the amount of Ω_{c0} decreases.

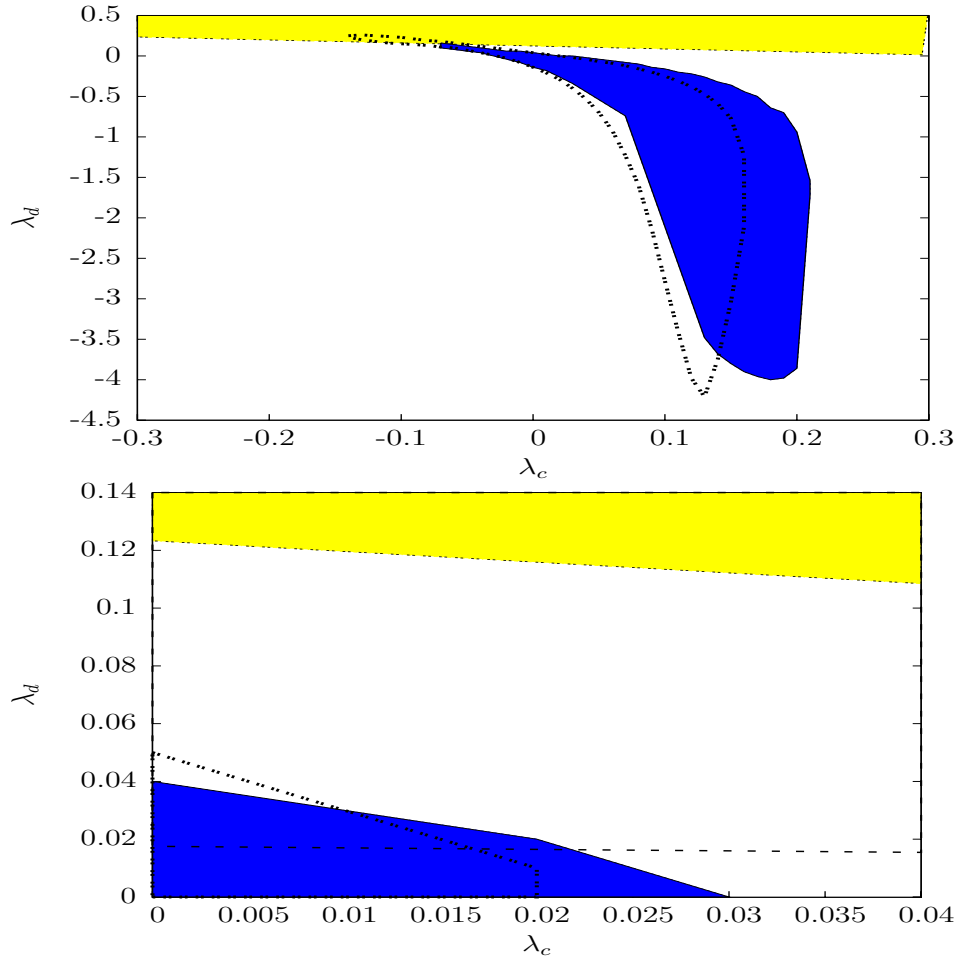


Figure 2. A region of parameters λ_d and λ_c for which the cosmic evolution has a late time attractor (the yellow regions above the dashed lines), and the 99.7% confidence levels from the combined analysis of SNIa data, CMB shift parameter and BAO measurement. The upper panel shows the case of arbitrary λ_d and λ_c , while the lower panel shows the case where $\lambda_d, \lambda_c \geq 0$. The blue regions represent the confidence regions for the case that includes baryons and prior $\Omega_{b0} = 0.047 \pm 0.006$, while the thick dotted lines represent the confidence levels for the case where baryons are neglected. The dashed lines are plotted by setting $\Omega_{cc} = 0.27$, but the thick dashed line in the lower panel is plotted by setting $\Omega_{cc} = 0.05$. We note that the region above the thick dashed line also represents the region for which the cosmic evolution has attractor.

We now consider the case of arbitrary λ_d and λ_c . We also perform a χ^2 fit for the

case with baryons and without baryons. For the case where baryons are neglected, it follows from figure 2 that the attractor can occur at present ($\Omega_{cc} \approx 0.3$) for a narrow range of λ_d and λ_c . Nevertheless, a small Ω_{cc} is required by observations if we restrict λ_d and λ_c to be positive. This implies that the attractor must occur in the future. Similarly to the case of $\lambda_d = \lambda_c = b^2$, the attractor cannot be reached at present if baryons are included in the consideration. Nevertheless, for suitable values of λ_c and λ_d which satisfy the observational constraints, the attractor in this case can be reached faster than the case of $\lambda_c = \lambda_d$.

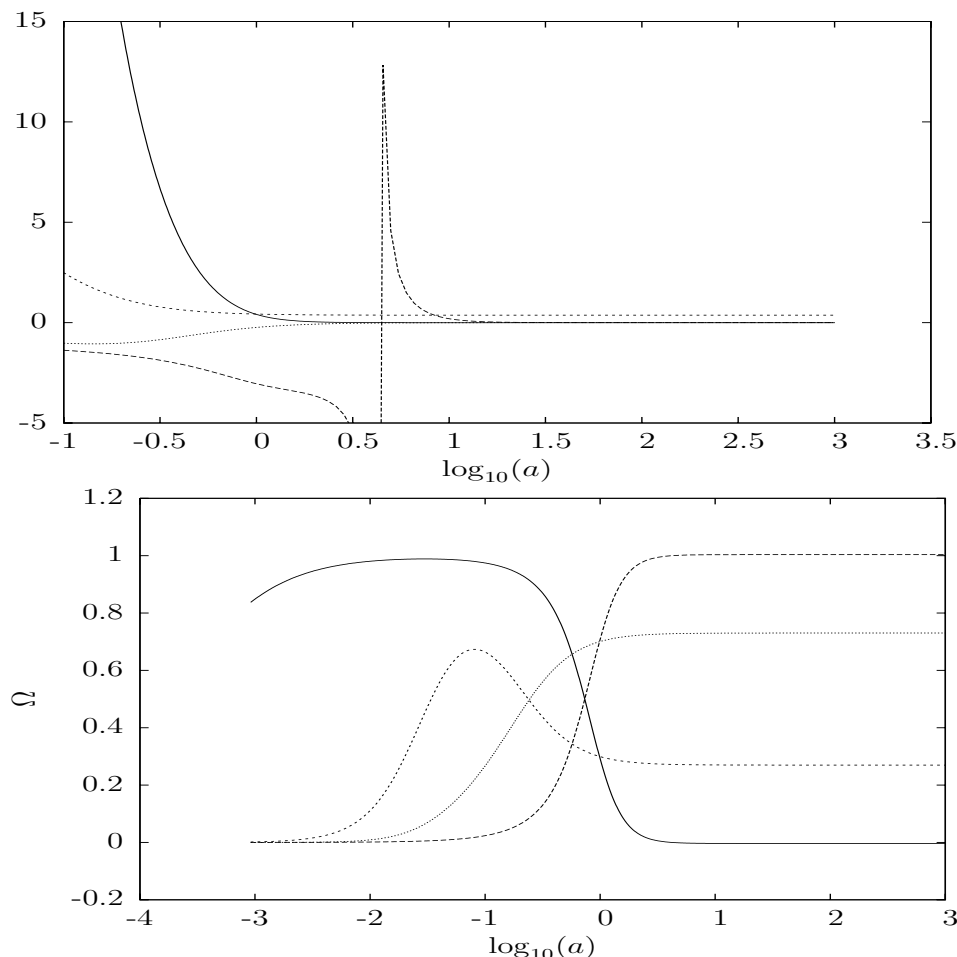


Figure 3. The upper panel shows the evolution of r (solid and dashed lines) and $\dot{r}/(rH)$ (long dashed and dotted lines), while the lower panel shows the evolution of Ω_c (solid and dashed lines) and Ω_d (long dashed and dotted lines). The solid and long dashed lines correspond to the case where the value of b^2 , c and Ω_{c0} equal to their best fit value, while the dashed and dotted lines correspond to the case where b^2 is chosen such that Ω_{cc} is close to Ω_{c0} , i.e. $\Omega_{cc} = 0.27$.

In order to check whether the cosmic coincidence can be alleviated for this form of interaction, we study the evolution of r during the present epoch. Since the evolution of r for the case with baryons and without baryons have nearly the same feature, we consider only the latter case. We first consider the case where $b^2 = \lambda_c = \lambda_d$. Setting b^2 ,

c and Ω_{c0} equal to their best fit value, i.e. $b^2 = -0.004$, $c = 0.84$ and $\Omega_{c0} = 0.3$, the evolution of r and $r' = \dot{r}/(rH)$ is plotted in figure 3. From figure 3, we see that $|r'| > 1$ during the present epoch because Ω_{c0} is quite different from Ω_{cc} . Due to a negative b^2 , r and Ω_c become negative and consequently reach the attractor at late time. Recall that $\Omega_c > 0$ at attractor if $b^2 \geq \Omega_{cc}/3$. To solve the coincidence problem, the ratio r should vary slowly during the present epoch such that $|r'| \lesssim 1$ today [4]. The present value of $|r'|$ will decrease if the value of Ω_{cc} gets closer to the value of Ω_{c0} , i.e. the cosmic evolution reaches the attractor near the present. According to the yellow region in figure 1, the value of Ω_{cc} will increase and get closer to Ω_{c0} if b^2 increases. However, $|r'|$ during the present epoch will be smaller than 1 only when b^2 is larger than the observational bound. The evolution of r for the case where Ω_{cc} is close to Ω_{c0} is shown in figure 3. In this case, the value of c and Ω_{c0} is the best fit value, while the value of b^2 is larger than the observational bound but is inside the yellow region in figure 1. From figure 3 we see that $|r'| < 1$ during the present epoch in this case but the amount of Ω_c during the early time is too small. For this reason, this case does not satisfy the observational constraints. Hence, in the case of $\lambda_c = \lambda_d$, the coincidence problem is not really alleviated for this form of interaction terms.

Next, we consider the case where $\lambda_c \neq \lambda_d$. We first set c , λ_c , λ_d and Ω_{c0} equal to their best fit value, i.e. $c = 0.37$, $\lambda_c = 0.08$, $\lambda_d = -0.45$ and $\Omega_{c0} = 0.27$. This choice of the parameter value is outside the yellow region in figure 2. Since the interaction term Q is dominated by $3H\lambda_d\Omega_d$ during the present epoch, Q becomes negative at present. Hence, r and also Ω_c become negative and consequently reach the attractor at late time. Of course, the attractor in this case does not correspond to the physical attractor. The evolution of r and Ω_c is shown in figure 4. Similarly to the case of $\lambda_c = \lambda_d$, the present value of $|r'|$ for this choice of parameters value is larger than 1 because Ω_{cc} is quite different from Ω_{c0} . We now keep Ω_{c0} fixed and choose the new value of parameters c , λ_c and λ_d such that it satisfies the observational constraints and the cosmic attractor occurs at $\Omega_{cc} = 0.24$ near the present epoch. This choice of the parameters value is inside the intersection between the yellow region and the confidence region in figure 2. From figure 4, we see that the present value of $|r'|$ is smaller than 1 and the attractor is reached near the present epoch for this choice of the parameters value. Based on soft coincidence idea, the coincidence problem can be alleviated in this case. The coincidence problem is better alleviated if $\Omega_{cc} = \Omega_{c0}$ or equivalently if the cosmic attractor is reached at the present. Unfortunately, the parameter values that make $\Omega_{cc} = \Omega_{c0}$ do not satisfy the observational constraints. The evolution of r and Ω_c for this case is shown in figure 4. From the figure, it is clear that this case is ruled out by observations. We note that the present value of $|r'|$ will increase if we include baryons in the above consideration.

Finally, we estimate whether $|r'|$ can be smaller than 1 at present if we constrain the parameters of dark energy by SDSS matter power spectrum. Here, we will not perform a complete fit for this dataset because the nature of the perturbations in holographic dark energy is not yet completely understood. To write down the evolution equations for the density perturbation and compute the matter power spectrum for this interacting

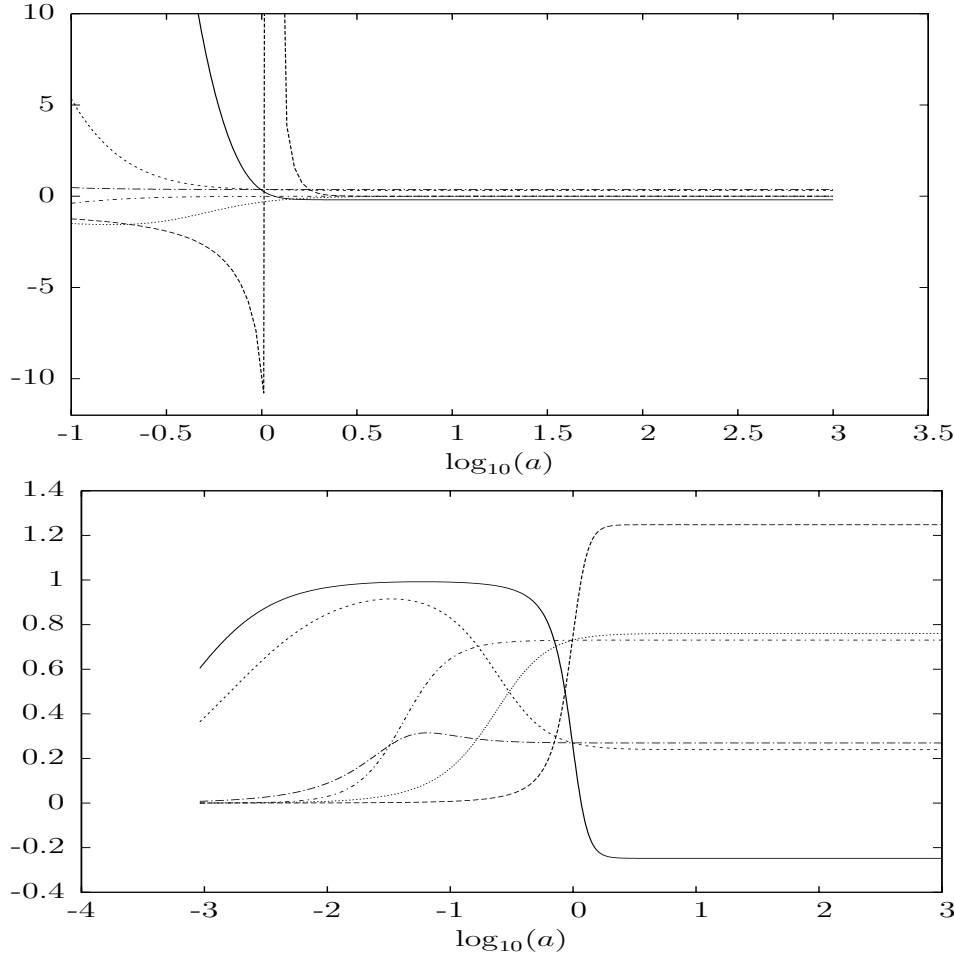


Figure 4. The upper panel shows the evolution of r (solid, dashed and long dashed dotted lines) and $\dot{r}/(rH)$ (long dashed, dotted and dashed dotted lines), while the lower panel shows the evolution of Ω_c (solid, dashed and long dashed dotted lines) and Ω_d (long dashed, dotted and dashed dotted lines). The solid and long dashed lines correspond to the case where the value of λ_c , λ_d , c and Ω_{c0} equal to their best fit value, the dashed and dotted lines correspond to the case where c , λ_c and λ_d are chosen such that Ω_{cc} is close to Ω_{c0} , i.e. $\Omega_{cc} = 0.24$, and the long dashed dotted and dashed dotted lines correspond to the case where c , λ_c and λ_d are chosen such that $\Omega_{cc} = \Omega_{c0}$.

dark energy model, we use the assumption below. From the results in [22], we suppose that the perturbation in holographic dark energy can be neglected when $kR_e/a \gg 1$, where k is the wavenumber of the perturbation modes. Using eqs. (1) and (6) and supposing that radiation can be neglected during matter domination, one can show that $H^{-1}/R_e = \sqrt{\Omega_d}/c$, i.e. the Hubble radius is smaller than the event horizon if $\sqrt{\Omega_d} < c$. Since we use the data from SDSS which measures the matter power spectrum on scales smaller than the Hubble radius, we neglect the perturbation in holographic dark energy in the calculation of the matter power spectrum. We write the perturbed interaction term using the formulas in [23, 24], so that the evolution equations for the

perturbation in CDM are

$$\begin{aligned}\frac{d\Delta_c}{d\eta} &= -kV_c + 3\mathcal{H}\Psi \left(\lambda_c + \lambda_d \frac{\rho_d}{\rho_c} \right) - 3\frac{d\Phi}{d\eta} \left(\lambda_c + \lambda_d \frac{\rho_d}{\rho_c} \right) - 3\mathcal{H}\lambda_d \Delta_c \frac{\rho_d}{\rho_c}, \\ \frac{dV_c}{d\eta} &= -\mathcal{H}V_c + k\Psi,\end{aligned}\tag{41}$$

where Δ_c and V_c are the gauge-invariant density contrast and velocity perturbation of CDM, Ψ and Φ are the metric perturbation, $\mathcal{H} = a^{-1}(da/d\eta)$ and η is the conformal time. We solve the above equations, compute the matter power spectrum and compare the obtained matter power spectrum with SDSS data using CMBEASY [25]. By checking the value of χ^2 , we have found that the best fit parameters for this dataset are different from the best fit parameters from the observational constraints on the homogeneous universe. Instead of searching for the best fit parameters for this dataset, we roughly check the viability of the parameters by comparing the matter power spectrum of the considered models with the matter power spectrum of Λ CDM model whose parameters are taken from the best fit value of 3-year WMAP and SDSS data [26]. In figure 5, we plot the fractional difference of the matter power spectrum between interacting holographic dark energy and Λ CDM model. From this figure, we see that for suitable ranges of dark energy parameters, $|r'|$ can be smaller than 1 at present and the difference of the matter power spectrum can be smaller than the error for the matter power spectrum of SDSS data. This implies that the alleviation of the coincidence problem by this interacting dark energy model is not excluded by SDSS data.

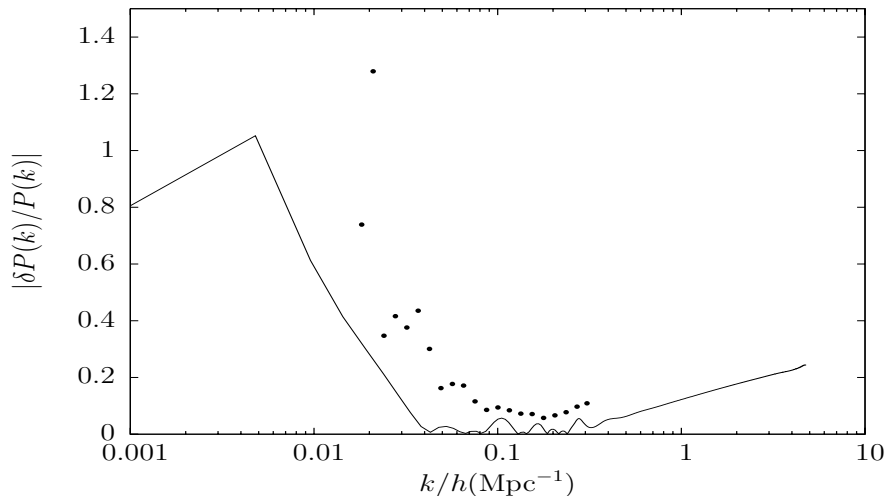


Figure 5. The fractional difference of the matter power spectrum $|\delta P(k)/P(k)|$ between interacting holographic dark energy and Λ CDM model. For this plot, the parameters of dark energy are chosen such that $|r'| \approx 0.9$ at present. The fractional error for the matter power spectrum $|\delta P(k)/P(k)| = \text{error} / \text{spectrum}$ of SDSS data is represented by dots.

5. Conclusions

For the interacting holographic dark energy model, we study the fixed points and their stability, and compare a range of model parameters for which attractor exists with the 99.7% confidence levels from the combined analysis of SNIa data, CMB shift parameter and BAO measurement. Neglecting baryons, the observational constraints require that the value of Ω_c at the attractor point must be small if $\lambda_d = \lambda_c$ or $\lambda_d, \lambda_c > 0$. This implies that the cosmic evolution will reach the attractor point in the future when Ω_c becomes small. In this case, r cannot be slowly varying during the present epoch and the cosmic attractor cannot be reached near the present. Hence, the coincidence problem is not really alleviated for this case. However, if λ_d and λ_c are allowed to be negative, the cosmic evolution can reach the attractor near the present epoch for a narrow range of λ_d and λ_c . Therefore, the coincidence problem is possible to alleviate in this case. Including baryons in our consideration, the attractor of the cosmic evolution cannot occur at present due to the non-vanishing baryon fraction. According to observations, the fixed point in this case is possible only when Q is small and positive. Hence, the fixed point will be slowly reached in the future. These results indicate that for the interacting holographic dark energy model with the interaction terms considered here, the cosmic coincidence problem cannot be alleviated very well. We also briefly considered the constraint from SDSS matter power spectrum on the dark energy parameters. We have found that the parameters ranges that lead to the alleviation of cosmic coincidence are allowed by SDSS data.

Acknowledgments

The author would like to thank Bin Wang for helpful discussions and suggestions and for hospitality at Fudan University during the final stage of this work. He also thanks A. Ungkitchanukit and anonymous referee for comments on the manuscript. The observational fitting was performed using the workstation of the Biophysics group, Kasetsart University. This work is supported by Thailand Research Fund (TRF) and vcharkarn.com.

References

- [1] Riess A G *et al*, *Observational evidence from supernovae for an accelerating universe and a cosmological constant*, 1998 *Astron. J.* **116** 1009 [arXiv:astro-ph/9805201]
- [2] Perlmutter S *et al*, *Measurements of Omega and Lambda from 42 high-redshift supernovae* 1999 *Astrophys. J.* **517** 565 [arXiv:astro-ph/9812133]
- [3] Zimdahl W and Pavón D, *Scaling cosmology*, 2003 *Gen. Rel. Grav.* **35** 413 [arXiv:astro-ph/0210484]
- [4] del Campo S, Herrera R, Olivares G and Pavón D, *Interacting models of soft coincidence*, 2006 *Phys. Rev.* **D74** 023501 [arXiv:astro-ph/0606520]
- [5] Sadjadi H M and Alimohammadi M, *Cosmological coincidence problem in interacting dark energy models*, 2006 *Phys. Rev.* **D74** 103007 [arXiv:gr-qc/0610080]

- [6] Amendola L, *Coupled quintessence*, 2000 *Phys. Rev.* **D62** 043511 [[arXiv:astro-ph/9908023](#)]
- [7] Chimento L P, Jakubi A S, Pavón D and Zimdahl W, *Interacting quintessence solution to the coincidence problem*, 2003 *Phys. Rev.* **D67** 083513 [[arXiv:astro-ph/0303145](#)]
- [8] Cohen A G, Kaplan D B and Nelson A E, *Effective field theory, black holes, and the cosmological constant*, 1999 *Phys. Rev. Lett.* **82** 4971 [[arXiv:hep-th/9803132](#)]
- [9] Li M, *A model of holographic dark energy*, 2004 *Phys. Lett.* **B603** 1 [[arXiv:hep-th/0403127](#)]
- [10] Setare M R and Vagenas E C, *The cosmological dynamics of interacting holographic dark energy model*, 2007 [[arXiv:0704.2070](#)]
- [11] Setare M R, *Interacting holographic dark energy model in non-flat universe*, 2006 *Phys. Lett.* **B642** 1 [[arXiv:hep-th/0609069](#)]
- [12] Setare M R, *Bulk-brane interaction and holographic dark energy*, 2006 *Phys. Lett.* **B642** 421 [[arXiv:hep-th/0609104](#)]
- [13] Setare M R, *Interacting holographic phantom*, 2007 *Eur. Phys. J.* **C50** 991 [[arXiv:hep-th/0701085](#)]
- [14] Elizalde E, Nojiri S, Odintsov S D and Wang P, *Dark energy: vacuum fluctuations, the effective phantom phase, and holography*, 2005 *Phys. Rev.* **D71** 103504 [[arXiv:hep-th/0502082](#)]
- [15] Gong Y, Wang B and Wang A, *Thermodynamical properties of dark energy*, 2007 *Phys. Rev.* **D75** 123516 [[arXiv:gr-qc/0611155](#)]
- [16] Riess A G *et al*, *New Hubble Space Telescope discoveries of type Ia supernovae at $z \lesssim 1$: narrowing constraints on the early behavior of dark energy*, 2006 [[arXiv:astro-ph/0611572](#)]
- [17] Wang Y and Mukherjee P, *Observational constraints on dark energy and cosmic curvature*, 2006 *Astrophys. J.* **650** 1 [[arXiv:astro-ph/0703780](#)]
- [18] Eisenstein D J *et al*, *Detection of the baryon acoustic peak in the large-scale correlation function of SDSS luminous red galaxies*, 2005 *Astrophys. J.* **633** 560 [[arXiv:astro-ph/0501171](#)]
- [19] Zhang X and Wu F, *Constraints on holographic dark energy from type Ia supernova observations*, 2005 *Phys. Rev.* **D72** 043524 [[arXiv:astro-ph/0506310](#)]
- [20] Zhang X and Wu F, *Constraints on holographic dark energy from latest supernovae, Galaxy Clustering, and Cosmic Microwave Background Anisotropy Observations*, 2007 *Phys. Rev.* **D76** 023502 [[arXiv:astro-ph/0701405](#)]
- [21] Spergel D N *et al*, *First year Wilkinson Microwave Anisotropy Probe (WMAP) observations: determination of cosmological parameters*, 2003 *Astrophys. J. Suppl.* **148** 175 [[arXiv:astro-ph/0302209](#)]
- [22] Li M, Lin C and Wang Y, *Some issues concerning holographic dark energy*, 2008 [[arXiv:0801.1407](#)]
- [23] Kodama H and Sasaki M, *Cosmological perturbation theory*, 1984 *Prog. Theor. Phys. Suppl.* **78** 1
- [24] Malik K, *Cosmological perturbations in an inflationary universe*, 2001 [[arXiv:astro-ph/0101563](#)]
- [25] Doran M, *Cmbeasy:: an object oriented code for the cosmic microwave background*, 2005 *JCAP* **0510** 011 [[arXiv:astro-ph/0302138](#)]
- [26] Spergel D N *et al*, *Wilkinson Microwave Anisotropy Probe (WMAP) three year results: implications for cosmology*, 2007 *Astrophys. J. Suppl.* **170** 377 [[arXiv:astro-ph/0603449](#)]